Erratum: Strange and multistrange particle production in Au+Au collisions at $\sqrt{s_{NN}} = 62.4$ GeV [Phys. Rev. C 83, 024901 (2011)]

M. M. Aggarwal, Z. Ahammed, A. V. Alakhverdyants, I. Alekseev, J. Alford, B. D. Anderson, C. D. Anson, D. Arkhipkin, G. S. Averichev, J. Balewski, D. R. Beavis, R. Bellwied, M. J. Betancourt, R. R. Betts, A. Bhasin, A. K. Bhati, H. Bichsel, J. Bielcik, J. Bielcikova, B. Biritz, L. C. Bland, W. Borowski, J. Bouchet, E. Braidot, A. V. Brandin, A. Bridgeman, S. G. Brovko, E. Bruna, S. Bueltmann, I. Bunzarov, T. P. Burton, X. Z. Cai, H. Caines, M. Calderón de la Barca Sánchez, D. Cebra, R. Cendejas, M. C. Cervantes, Z. Chajecki, P. Chaloupka, S. Chattopadhyay, H. F. Chen, J. H. Chen, J. Y. Chen, J. Cheng, M. Cherney, A. Chikanian,* K. E. Choi, W. Christie, P. Chung, M. J. M. Codrington, R. Corliss, J. G. Cramer, H. J. Crawford, S. Dash, A. Davila Leyva, L. C. De Silva, R. R. Debbe, T. G. Dedovich, A. A. Derevschikov, R. Derradi de Souza, L. Didenko, P. Djawotho, S. M. Dogra, X. Dong, J. L. Drachenberg, J. E. Draper, J. C. Dunlop, M. R. Dutta Mazumdar, L. G. Efimov, M. Elnimr, J. Engelage, G. Eppley, M. Estienne, L. Eun, O. Evdokimov, R. Fatemi, J. Fedorisin, R. G. Fersch, E. Finch, V. Fine, Y. Fisyak, C. A. Gagliardi, D. R. Gangadharan, A. Geromitsos, F. Geurts, P. Ghosh, Y. N. Gorbunov, A. Gordon, O. Grebenyuk, D. Grosnick, S. M. Guertin, A. Gupta, W. Guryn, B. Haag, O. Hajkova, A. Hamed, L-X. Han, J. W. Harris, J. P. Hays-Wehle, M. Heinz, S. Heppelmann, A. Hirsch, E. Hjort, G. W. Hoffmann,* D. J. Hofman, B. Huang, H. Z. Huang, T. J. Humanic, L. Huo, G. Igo,* P. Jacobs, W. W. Jacobs, C. Jena, F. Jin, J. Joseph, E. G. Judd, S. Kabana, K. Kang, J. Kapitan, K. Kauder, D. Keane, A. Kechechyan, D. Kettler, D. P. Kikola, J. Kiryluk, A. Kisiel, V. Kizka, S. R. Klein, A. G. Knospe, D. D. Koetke, T. Kollegger, J. Konzer, I. Koralt, L. Koroleva, W. Korsch, L. Kotchenda, V. Kouchpil, P. Kravtsov, K. Krueger, M. Krus, L. Kumar, P. Kurnadi, M. A. C. Lamont, J. M. Landgraf, S. LaPointe, J. Lauret, A. Lebedev, R. Lednicky, J. H. Lee, W. Leight, M. J. LeVine, C. Li, L. Li, N. Li, W. Li, X. Li, X. Li, Y. Li, Z. M. Li, M. A. Lisa, F. Liu, H. Liu, J. Liu, T. Ljubicic, W. J. Llope, R. S. Longacre, W. A. Love,* Y. Lu, E. V. Lukashov, X. Luo, G. L. Ma, Y. G. Ma, D. P. Mahapatra, R. Majka,* O. I. Mall, L. K. Mangotra, R. Manweiler, S. Margetis, C. Markert, H. Masui, H. S. Matis, Yu. A. Matulenko, D. McDonald, T. S. McShane,* A. Meschanin, R. Milner, N. G. Minaev, S. Mioduszewski, A. Mischke, M. K. Mitrovski, B. Mohanty, M. M. Mondal, B. Morozov, D. A. Morozov, M. G. Munhoz, M. Naglis, B. K. Nandi, T. K. Nayak, P. K. Netrakanti, M. J. Ng, T. Niida, L. V. Nogach, S. B. Nurushev, G. Odyniec, A. Ogawa, K. Oh, A. Ohlson, V. Okorokov, E. W. Oldag, D. Olson, M. Pachr, B. S. Page, S. K. Pal, Y. Pandit, Y. Panebratsev, T. Pawlak, H. Pei, T. Peitzmann, C. Perkins, W. Peryt, S. C. Phatak, P. Pile, M. Planinic, M. A. Ploskon, J. Pluta, D. Plyku, N. Poljak, A. M. Poskanzer,* B. V. K. S. Potukuchi, C. B. Powell, D. Prindle, C. Pruneau, N. K. Pruthi, P. R. Pujahari, J. Putschke, H. Qiu, R. Raniwala, S. Raniwala, R. L. Ray, R. Redwine, R. Reed, H. G. Ritter, J. B. Roberts,* O. V. Rogachevskiy, J. L. Romero, A. Rose, L. Ruan, J. Rusnak, S. Sakai, I. Sakrejda, T. Sakuma, S. Salur, J. Sandweiss,* E. Sangaline, S. Sato, J. Schambach, R. P. Scharenberg, A. M. Schmah, N. Schmitz, T. R. Schuster, J. Seele, J. Seger, I. Selyuzhenkov, P. Seyboth, E. Shahaliev, M. Shao, M. Sharma, S. S. Shi, E. P. Sichtermann, F. Simon, R. N. Singaraju, M. J. Skoby, N. Smirnov, P. Sorensen, J. Speltz, H. M. Spinka,* B. Srivastava, T. D. S. Stanislaus, D. Staszak, S. G. Steadman, J. R. Stevens, R. Stock, M. Strikhanov, B. Stringfellow, A. A. P. Suaide, M. C. Suarez, N. L. Subba, M. Sumbera, X. M. Sun, Y. Sun, Z. Sun, B. Surrow, D. N. Svirida, T. J. M. Symons, A. Szanto de Toledo, J. Takahashi, A. H. Tang, Z. Tang, L. H. Tarini, T. Tarnowsky, D. Thein, J. H. Thomas, J. Tian, A. R. Timmins, D. Tlusty, T. Todoroki, M. Tokarev, T. A. Trainor, V. N. Tram, S. Trentalange, R. E. Tribble, P. Tribedy, O. D. Tsai, T. Ullrich, D. G. Underwood, G. Van Buren, G. van Nieuwenhuizen, J. A. Vanfossen, Jr., R. Varma, G. M. S. Vasconcelos, A. N. Vasiliev, F. Videbæk, Y. P. Viyogi, S. Vokal, S. A. Voloshin, M. Wada, M. Walker, F. Wang, G. Wang, H. Wang, J. S. Wang, Q. Wang, X. L. Wang, Y. Wang, G. Webb, J. C. Webb, G. D. Westfall, C. Whitten, Jr., H. Wieman, S. W. Wissink, R. Witt, W. Witzke, Y. F. Wu, W. Xie, H. Xu, N. Xu, Q. H. Xu, W. Xu, Y. Xu, Z. Xu, L. Xue, Y. Yang, P. Yepes, K. Yip, I-K. Yoo, Q. Yue, M. Zawisza, H. Zbroszczyk, W. Zhan, J. B. Zhang, S. Zhang, W. M. Zhang, X. P. Zhang, Y. Zhang, Z. P. Zhang, J. Zhao, C. Zhong, W. Zhou, X. Zhu, Y. H. Zhu, R. Zoulkarneev, and Y. Zoulkarneeva
(STAR Collaboration)

(Received 8 March 2023; published 24 April 2023)

DOI: 10.1103/PhysRevC.107.049903

In this erratum, we correct the reported results of K_S^0 meson and Λ, Ξ, and Ω baryon production in Au+Au collisions at $\sqrt{s_{NN}} = 62.4$ GeV.

In Fig. 3 of the original article, there were multiple issues as follows:

(i) the data point at transverse momentum $p_T = 5.5$ GeV/c for K_S^0 in 0%–5% central collisions was not plotted;

*Deceased.

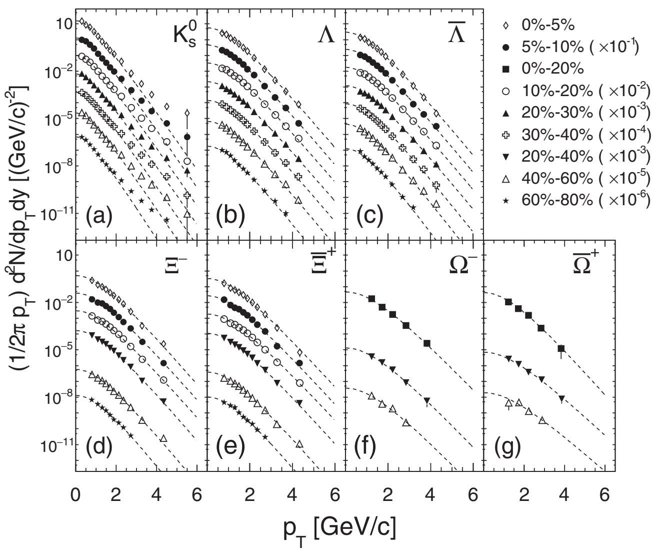

FIG. 3. Efficiency-corrected p_T spectra for the indicated particle types and centrality bins in Au+Au collisions at $\sqrt{s_{NN}} = 62.4$ GeV. Note that seven centrality bins have been used for K_S^0 and Λ while only six and three have been used for Ξ and Ω, respectively. Only statistical uncertainties are shown. The Λ spectra are corrected for the feed-down from Ξ decay. The dashed lines are fits to the p_T spectra with a Maxwell-Boltzmann function.

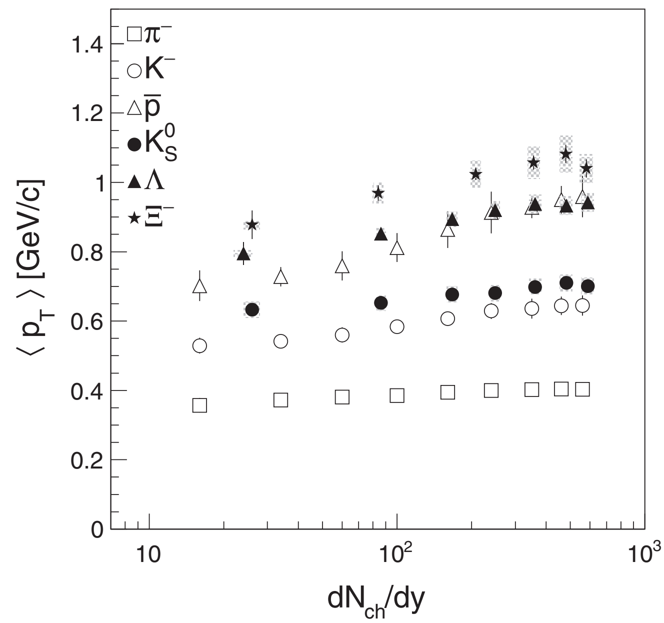

FIG. 4. Extrapolated average transverse momenta $\langle p_T \rangle$ as a function of $dN_{\rm ch}/dy$ for different particle species in Au+Au collisions at $\sqrt{s_{NN}} = 62.4$ GeV. Statistical uncertainties are represented by the bars while the systematic uncertainties are represented by the gray bands. The π^-, K^-, and $\bar{p}$ data were extracted from Ref. [1]. Some data points are shifted in the horizontal direction for visibility.

(ii) the p_T spectra for Λ and $\bar{\Lambda}$ were not corrected for the feed-down contributions from charged and neutral Ξ decays, inconsistent with the descriptions in the text and figure caption;

(iii) the data points at $p_T = 4.34$ GeV/c for both Ξ^- and $\bar{\Xi}^+$ in 0%–5% and 40%–60% central collisions were not plotted;

(iv) the p_T spectra for Ω^- and $\bar{\Omega}^+$ in 20%–40% and 40%–60% central Au+Au collisions were mistakenly plotted with 10 and 100 times larger multiplicative factors, respectively.

Figure 3 in this erratum shows the p_T spectra with these issues corrected.

In the following of this erratum, we obtain the total integrated yield dN/dy and mean transverse momentum $\langle p_T \rangle$ via the fits to the p_T spectra with the Maxwell-Boltzmann function $\frac{d^2N}{2\pi p_T dp_T dy} \propto m_T e^{-\frac{m_T}{T}}$ and the exponential function $\frac{d^2N}{2\pi p_T dp_T dy} \propto e^{-\frac{m_T}{T}}$, following the same method described in the original article. Note that, while the original article stated that all the particle species were fit in $p_T < 1.5$ GeV/c, the actual fit range for Ξ^- and $\bar{\Xi}^+$ was $p_T < 2.0$ GeV/c and that for Ω^- and $\bar{\Omega}^+$ was $p_T < 2.5$ GeV/c.

In Table IV of the original article, there was a mistake in the calculation of $\langle p_T \rangle$ and its statistical uncertainty for all the particle species. In Table IV of this erratum, we present corrected $\langle p_T \rangle$ for these particles obtained from the fits to the p_T spectra shown in Fig. 3 of this erratum.

In Fig. 4 of the original article, incorrect $\langle p_T \rangle$ as a function of the midrapidity charged-particle yield $dN_{\rm ch}/dy$ was plotted for K_S^0, Λ, and Ξ^- because of the aforementioned reason in Table IV. Figure 4 of this erratum shows corrected $\langle p_T \rangle$ as a function of $dN_{\rm ch}/dy$ for K_S^0, Λ, and Ξ^-. The $\langle p_T \rangle$ for π^-, K^-, and $\bar{p}$ remains unchanged. The overall hierarchy of $\langle p_T \rangle$ among the hadron species does not change.

TABLE IV. Average transverse momenta, $\langle p_T \rangle$, in GeV/c, for the strange hadrons from Au+Au collisions at $\sqrt{s_{NN}} = 62.4$ GeV. The first uncertainty is statistical, while the second is the systematic uncertainty arising from the extrapolation in the low p_T region.

	K_S^0	Λ	$\bar{\Lambda}$	Ξ^-	$\bar{\Xi}^+$
0%–5%	0.701 ± 0.008 ± 0.024	0.942 ± 0.016 ± 0.027	0.916 ± 0.015 ± 0.024	1.040 ± 0.026 ± 0.041	1.055 ± 0.036 ± 0.047
5%–10%	0.710 ± 0.008 ± 0.024	0.933 ± 0.018 ± 0.027	0.924 ± 0.016 ± 0.026	1.082 ± 0.026 ± 0.053	1.049 ± 0.035 ± 0.046
10%–20%	0.698 ± 0.007 ± 0.024	0.938 ± 0.014 ± 0.027	0.919 ± 0.012 ± 0.026	1.057 ± 0.020 ± 0.046	1.067 ± 0.025 ± 0.049
20%–30%	0.681 ± 0.009 ± 0.024	0.920 ± 0.015 ± 0.025	0.923 ± 0.013 ± 0.027	1.023 ± 0.016 ± 0.040	1.008 ± 0.021 ± 0.034
30%–40%	0.677 ± 0.009 ± 0.023	0.894 ± 0.018 ± 0.022	0.877 ± 0.016 ± 0.021		
40%–60%	0.653 ± 0.009 ± 0.023	0.852 ± 0.018 ± 0.016	0.831 ± 0.016 ± 0.013	0.969 ± 0.022 ± 0.029	0.999 ± 0.026 ± 0.040
60%–80%	0.633 ± 0.014 ± 0.023	0.795 ± 0.033 ± 0.010	0.782 ± 0.029 ± 0.010	0.878 ± 0.041 ± 0.013	0.898 ± 0.054 ± 0.020

TABLE V. Integrated yield, dN/dy, for K_S^0, Λ, and $\overline{\Lambda}$ measured in Au+Au collisions at $\sqrt{s_{NN}} = 62.4$ GeV using data and a Maxwell-Boltzmann function for the extrapolation to the unmeasured low p_T region. Quoted uncertainties are the statistical and systematic uncertainties. The Λ and $\overline{\Lambda}$ yields are corrected by subtracting the contribution of the feed-down from the Ξ weak decays.

	K_S^0	Λ	$\overline{\Lambda}$
0%–5%	$27.4 \pm 0.6 \pm 2.9$	$14.8 \pm 0.4 \pm 2.2$	$7.8 \pm 0.2 \pm 1.0$
5%–10%	$21.9 \pm 0.5 \pm 2.3$	$12.2 \pm 0.3 \pm 1.9$	$6.1 \pm 0.1 \pm 0.8$
10%–20%	$17.1 \pm 0.3 \pm 1.7$	$9.1 \pm 0.2 \pm 1.3$	$4.7 \pm 0.1 \pm 0.6$
20%–30%	$12.1 \pm 0.3 \pm 1.1$	$6.2 \pm 0.1 \pm 0.8$	$3.11 \pm 0.06 \pm 0.42$
30%–40%	$8.1 \pm 0.2 \pm 0.7$	$4.1 \pm 0.1 \pm 0.6$	$2.25 \pm 0.04 \pm 0.30$
40%–60%	$4.0 \pm 0.1 \pm 0.3$	$2.01 \pm 0.04 \pm 0.26$	$1.16 \pm 0.02 \pm 0.16$
60%–80%	$1.13 \pm 0.05 \pm 0.09$	$0.532 \pm 0.024 \pm 0.074$	$0.322 \pm 0.014 \pm 0.034$

In the original article, the integrated yield dN/dy for Λ and $\bar{\Lambda}$ was obtained from the p_T spectra corrected for the feed-down contribution from the Ξ decays, however, incorrect values were copied in Table V for Λ in 0%–5% and 60%–80% central collisions and for $\bar{\Lambda}$ in 0%–5%, 20%–30%, and 60%–80% central collisions. Table V of this erratum shows the integrated yield dN/dy for Λ and $\bar{\Lambda}$ corrected for the feed-down contribution obtained from the fits to the p_T spectra shown in Fig. 3 of this erratum for such cases. The dN/dy for K_S^0 in Table V of this erratum remains unchanged compared to the original article.

The dN/dy for Ξ^-, $\bar{\Xi}^+$, Ω^-, and $\bar{\Omega}^+$ in Table VI of the original article is correct.

The results in Fig. 5 in the original article remain unchanged.

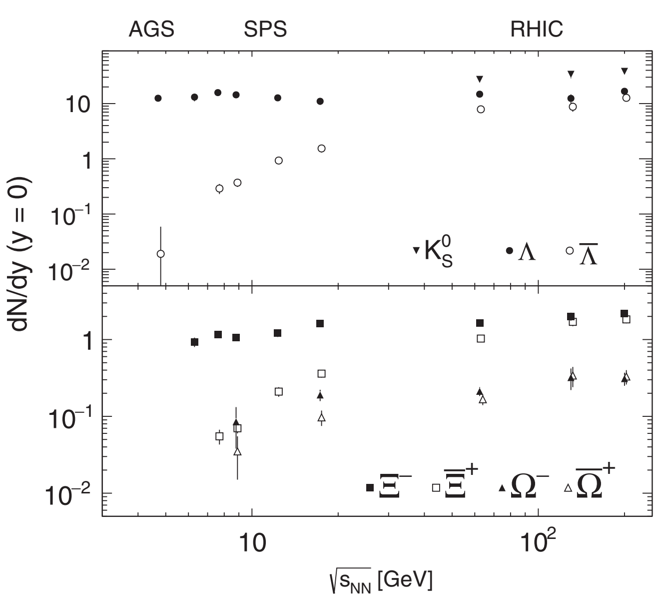

FIG. 6. Strange particle production yields at midrapidity in central Au+Au and Pb+Pb collisions versus the center of mass energy $\sqrt{s_{NN}}$. The top panel shows results for K_S^0 and Λ. The AGS values are from E896 [2] (centrality 0%–5%). The SPS values are from NA49 [3] (centrality 0%–7%) and the RHIC values are from STAR [4,5] (centrality 0%–5%). For the multistrange baryons Ξ and Ω (bottom panel), the SPS results are from NA57 [6] (centrality 0%–11%) and the RHIC values are from STAR [5,7] (centrality 0%–20%). The bars indicate only the statistical uncertainties for the STAR data points.

In Fig. 6 of the original article, incorrect dN/dy values were copied for Λ, $\bar{\Lambda}$, Ω^-, and $\bar{\Omega}^+$ at $\sqrt{s_{NN}}= 62.4$ GeV. Figure 6 of this erratum shows dN/dy as a function of $\sqrt{s_{NN}}$, where at $\sqrt{s_{NN}}= 62.4$ GeV, Λ, $\bar{\Lambda}$, Ω^-, and $\bar{\Omega}^+$ are plotted with correct central values and statistical uncertainties. The overall trend of dN/dy as a function of $\sqrt{s_{NN}}$ for these hadron species remains unchanged.

In Fig. 7 of the original article, incorrect ratios of antibaryon to baryon integrated yields were copied for Λ, $\bar{\Lambda}$, Ω^-, and $\bar{\Omega}^+$ at $\sqrt{s_{NN}}= 62.4$ GeV. Figure 7 of this erratum

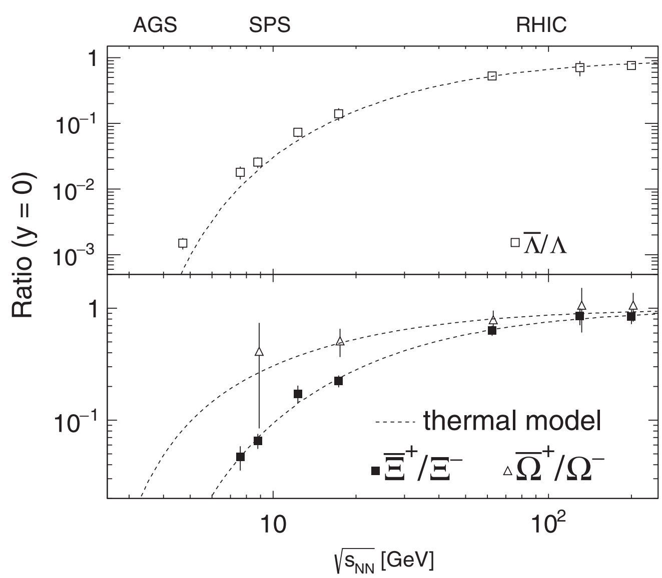

FIG. 7. Antibaryon to baryon yield ratios for strange baryons in central Au+Au and Pb+Pb collisions versus the center of mass energy $\sqrt{s_{NN}}$. $\overline{\Lambda}/\Lambda$ is shown in the top panel while ratios for the multistrange baryons are in the bottom panel. The data from AGS are not corrected for the weak decay feed-down from the multistrange baryons while the data from SPS and RHIC are corrected. The lines are the results of the thermal model calculation (see Sec. IV A of the original article). The AGS values are from E896 [2] (centrality 0%–5%). The SPS values are from NA49 [3] (centrality 0%–7%) and the RHIC values are from STAR [4,5] (centrality 0%–5%). For the multistrange baryons Ξ and Ω (bottom panel), the SPS results are from NA57 [6] (centrality 0%–11%), and the RHIC values are from STAR [5,7] (centrality 0%–20%). The bars indicate only the statistical uncertainties for the STAR data points.

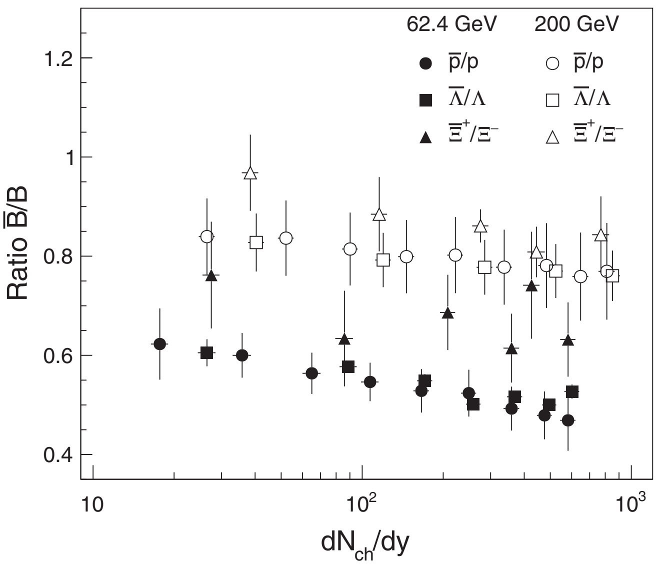

FIG. 8. Antibaryon to baryon yield ratios for strange particles and protons as a function of dN_{ch}/dy in Au+Au collisions at $\sqrt{s_{NN}} = 62.4$ and 200 GeV. The p data were extracted from Ref. [1]. The $\sqrt{s_{NN}} = 200$ GeV strange hadron data were extracted from Ref. [5]. Some data points are shifted in the horizontal direction for visibility. The bars indicate only the statistical uncertainties.

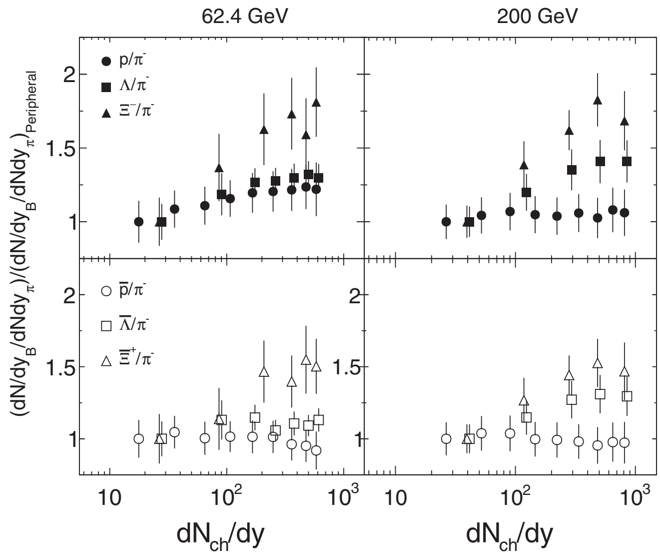

FIG. 12. Ratios of baryon (solid symbols) and antibaryon (open symbols) to π^- yield as a function of dN_{ch}/dy, normalized by the corresponding ratio in the most-peripheral collisions, in Au+Au collisions at $\sqrt{s_{NN}} = 62.4$ GeV (left panels) and $\sqrt{s_{NN}} = 200$ GeV (right panels). The π^- and p data were extracted from Ref. [1]. Some data points are shifted in the horizontal direction for visibility. The bars indicate only the statistical uncertainties.

shows the antibaryon to baryon ratio as a function of $\sqrt{s_{NN}}$, where at $\sqrt{s_{NN}}$= 62.4 GeV, Λ, $\bar{\Lambda}$, Ω^-, and $\bar{\Omega}^+$ are plotted with correct central values and statistical uncertainties. The overall trend of the antibaryon to baryon ratio as a function of $\sqrt{s_{NN}}$ for these hadron species remains unchanged.

In Fig. 8 of the original article, incorrect ratios of antibaryon to baryon integrated yields as a function of dN_{ch}/dy were copied for $\bar{\Lambda}/\Lambda$ at $\sqrt{s_{NN}}$= 62.4 GeV. Figure 8 of this erratum shows the antibaryon to baryon ratio as a function of dN_{ch}/dy, where at $\sqrt{s_{NN}}$= 62.4 GeV, $\bar{\Lambda}/\Lambda$ ratios are plotted with correct central values and statistical uncertainties. The overall trend of the antibaryon to baryon ratio as a function of dN_{ch}/dy at $\sqrt{s_{NN}}$= 62.4 GeV remains unchanged.

The results of the thermal model fit to the p_T spectra presented in Figs. 9 to 11 in the original article are found to be unchanged.

To quantify the baryon enhancement, the double ratio of (anti)baryon to π^- yields with respect to the most-peripheral bin was introduced. In Fig. 12 of the original article, the double ratios of Λ/π^-, $\bar{\Lambda}/\pi^-$, Ξ^-/π^-, and $\bar{\Xi}^+/\pi^-$ at $\sqrt{s_{NN}}$= 62.4 GeV had a mistake in their calculations, whereby the data in the most-peripheral bin deviated from unity. Figure 12 of this erratum shows the corrected double ratios for Λ/π^-, $\bar{\Lambda}/\pi^-$, Ξ^-/π^-, and $\bar{\Xi}^+/\pi^-$ at $\sqrt{s_{NN}}$= 62.4 GeV. The overall trend of the corrected double ratios at $\sqrt{s_{NN}}$= 62.4 GeV remains the same.

In Fig. 13 of the original article, incorrect ratios of (anti)baryon to π^- yields were copied for Λ/π^-, $\bar{\Lambda}/\pi^-$, Ξ^-/π^-, $\bar{\Xi}^+/\pi^-$, Ω^-/π^-, and $\bar{\Omega}^+/\pi^-$ at $\sqrt{s_{NN}}$= 62.4 GeV. Figure 13 of this erratum shows the (anti)baryon to π^- ratio as a function of $\sqrt{s_{NN}}$, where at $\sqrt{s_{NN}}$= 62.4 GeV, Λ/π^-, $\bar{\Lambda}/\pi^-$, Ξ^-/π^-, $\bar{\Xi}^+/\pi^-$, Ω^-/π^-, and $\bar{\Omega}^+/\pi^-$ are plotted

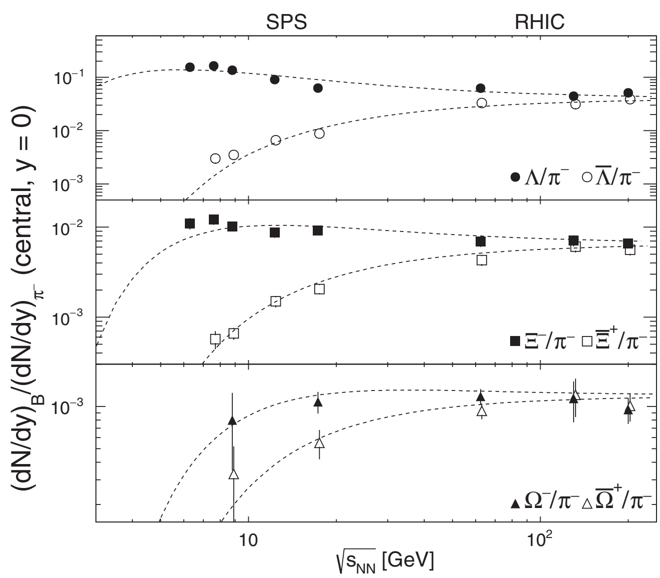

FIG. 13. Ratio of baryon (solid symbols) and antibaryon (open symbols) to π^- at midrapidity in central Au+Au and Pb+Pb collisions as a function of $\sqrt{s_{NN}}$. The lines are the results of the thermal model calculation (see Sec. IV A of the original article). The SPS values are from NA49 [3] (centrality 0%–7%) and the RHIC values are from STAR [4,5] (centrality 0%–5%). For the multistrange baryons Ξ and Ω (bottom panel), the SPS results are from NA57 [6] (centrality 0%–11%) and the RHIC values are from STAR [5,7] (centrality 0%–20%). The bars indicate only the statistical uncertainties for the STAR data points.

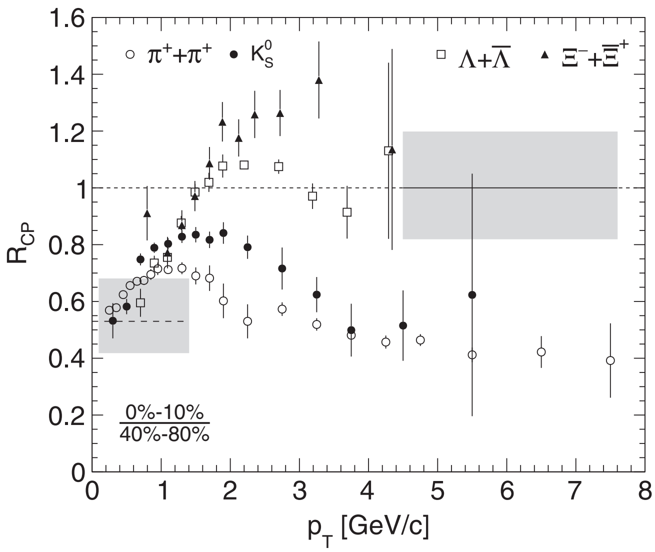

FIG. 14. Nuclear modification factor $R_{\rm CP}$, calculated as the ratio between 0%–10% central spectra and 40%–80% peripheral spectra, for π, K_S^0, Λ, and Ξ particles in Au+Au collisions at $\sqrt{s_{NN}} =$ 62.4 GeV. The π $R_{\rm CP}$ values were extracted from Ref. [8]. The vertical bars around the markers indicate only the statistical uncertainties. The gray band on the right side of the plot shows the uncertainty on the scaling by the number of binary collisions. The gray band on the lower left side indicates the uncertainty on the scaling by the number of participants. The solid and dashed lines inside these bands are the baselines of the scalings by the number of binary collisions and the number of participants, respectively.

with correct central values and statistical uncertainties. The overall trend of the (anti)baryon to π^- integrated yield ratio as a function of $\sqrt{s_{NN}}$ for these hadron species remains unchanged.

The suppression of strange hadrons is quantified by the nuclear modification factor $R_{\rm CP}$ as

$$R_{\rm CP} = \left[\frac{\frac{d^2N^{\rm central}}{dp_T\,dy}}{\frac{d^2N^{\rm peripheral}}{dp_T\,dy}}\right] \times \left[\frac{\langle N_{\rm bin}^{\rm peripheral}\rangle}{\langle N_{\rm bin}^{\rm central}\rangle}\right], \tag{1}$$

where $\langle N_{\rm bin}\rangle$ indicates the number of binary collisions in the Glauber model [9]. In Fig. 14 of the original article, $R_{\rm CP}$ between 0%–10% central spectra and 40%–80% peripheral spectra was calculated for $(\Lambda + \bar{\Lambda})$ not corrected for the feed-down contribution from the Ξ decays, and for $(\Xi^- + \bar{\Xi}^+)$ with a mistake in calculating p_T spectra in a wide centrality bin from those in narrow centrality bins. In this erratum, the p_T spectra for $(\Lambda + \bar{\Lambda})$ and $(\Xi^- + \bar{\Xi}^+)$ are recalculated using the corrected p_T spectra presented in Fig. 3 of this erratum. The p_T spectra in 0%–10% (40%–80%) central collisions are obtained by adding those in 0%–5% (40%–60%) and 5%–10% (60%–80%) central collisions with the centrality bin width as a weight. The $\langle N_{\rm bin}\rangle$ values used are listed in Table I of the original article. Using the same method as the p_T spectra, $\langle N_{\rm bin}\rangle$ in 0%–10% (40%–80%) central collisions is obtained by adding those in 0%–5% (40%–60%) and 5%–10% (60%–80%) central collisions with the centrality bin width as a weight. $R_{\rm CP}$ is calculated from the p_T spectra and $\langle N_{\rm bin}\rangle$ in 0%–10% and 40%–80% centrality collisions.

Figure 14 of this erratum shows $R_{\rm CP}$ for $(\Lambda + \bar{\Lambda})$ corrected for the feed-down contribution, and for $(\Xi^- + \bar{\Xi}^+)$ with the correct centrality merging method. The overall trend of $R_{\rm CP}$ for $(\Lambda + \bar{\Lambda})$ and $(\Xi^- + \bar{\Xi}^+)$ remains unchanged.

The results in Figs. 15 to 17 in the original article remain unchanged.

In summary, we have corrected the reported results of K_S^0, Λ, Ξ, and Ω production in Au+Au collisions at $\sqrt{s_{NN}}=$ 62.4 GeV. The overall trend of each figure does not change, and thus the physics conclusion of the original article remains the same.

We thank the RHIC Operations Group and RCF at BNL, the NERSC Center at LBNL, and the Open Science Grid consortium for providing resources and support. This work was supported in part by the offices of NP and HEP within the US DOE Office of Science; the US NSF; the Sloan Foundation; the DFG cluster of excellence "Origin and Structure of the Universe" of Germany; CNRS/IN2P3, FAPESP CNPq of Brazil; Ministry of Education and Science of the Russian Federation; NNSFC, CAS, MoST, and MoE of China; GA and MSMT of the Czech Republic; FOM and NWO of the Netherlands; DAE, DST, and CSIR of India; the Polish Ministry of Science and Higher Education, Korea Research Foundation; Ministry of Science, Education and Sports of the Republic of Croatia; and RosAtom of Russia.

[1] B. I. Abelev *et al.* (STAR Collaboration), Systematic measurements of identified particle spectra in *pp*, *d*+Au and Au+Au collisions from STAR, Phys. Rev. C **79**, 034909 (2009).

[2] H. Caines *et al.* (E896 Collaboration), An update on the strangeness production measurements and H_0 di-baryon search as performed by the AGS experiment 896, J. Phys. G: Nucl. Part. Phys. **27**, 311 (2001).

[3] T. Anticic *et al.* (NA49 Collaboration), Lambda and Anti-Lambda Production in Central Pb-Pb Collisions at 40-A-GeV, 80-A-GeV and 158-A-GeV, Phys. Rev. Lett. **93**, 022302 (2004).

[4] C. Adler *et al.* (STAR Collaboration), Midrapidity Lambda and Anti-Lambda Production in Au+Au Collisions at $\sqrt{s_{NN}} =$ 130 GeV, Phys. Rev. Lett. **89**, 092301 (2002).

[5] J. Adams *et al.* (STAR Collaboration), Scaling Properties of Hyperon Production in Au+Au Collisions at $\sqrt{s_{NN}} =$ 200-GeV, Phys. Rev. Lett. **98**, 062301 (2007).

[6] F. Antinori *et al.* (NA57 Collaboration), Energy dependence of hyperon production in nucleus nucleus collisions at SPS, Phys. Lett. B **595**, 68 (2004).

[7] J. Adams *et al.* (STAR Collaboration), Multistrange Baryon Production in Au-Au Collisions at $\sqrt{s_{NN}} =$ 130 GeV, Phys. Rev. Lett. **92**, 182301 (2004).

[8] B. I. Abelev *et al.* (STAR Collaboration), Energy dependence of $\pi^\pm$, p and $\bar{p}$ transverse momentum spectra for Au+Au collisions at $\sqrt{s_{NN}} =$ 62.4 and 200 GeV, Phys. Lett. B **655**, 104 (2007).

[9] M. L. Miller, K. Reygers, S. J. Sanders, and P. Steinberg, Glauber modeling in high energy nuclear collisions, Annu. Rev. Nucl. Part. Sci. **57**, 205 (2007).